



Fluoride sorption by zirconium (IV) loaded carboxylated orange peel

Ranjana Jha^a, Usha Jha^a, R.K. Dey^b, Sumit Mishra^a, S.K. Swain^{a,*}

^aDepartment of Applied Chemistry, Birla Institute of Technology, Mesra, Ranchi 835215, India

Tel. +91 651 2275444; email: skswain@bitmesra.ac.in

^bCentre for Applied Chemistry, Central University of Jharkhand, Ranchi 835205, India

Received 25 May 2013; Accepted 29 October 2013

ABSTRACT

The article reports on an investigation into the ability of zirconium (IV)-loaded carboxylated orange peel to remove the fluoride ion from drinking water and the parameters involved in this process. Various spectroscopic and microscopic techniques were used to characterize the adsorbent. The results suggested that the adsorbent exhibited reasonably significant fluoride removal over a wide range of pH value (3.0–8.0). The kinetic studies indicated that the adsorption process followed pseudo-second-order model. The adsorption isotherm has been modeled by the Langmuir, Freundlich, Temkin, and DR equation. The adsorption isotherm was well described by DR equation. The negative value of ΔG° and positive value of ΔH° revealed that the adsorption process was spontaneous and endothermic. The presence of NO_3^- , Cl^- , and SO_4^{2-} ions have negligible effect, whereas PO_4^{3-} and HCO_3^- retarded the fluoride removal capacity to some extent. The reuse study of the adsorbent resulted in retention of 83% capacity in 8th cycle. Desorption studies showed that the fluoride can easily be desorbed by using 0.1 N NaOH solution. The wide pH range, second-order kinetics, operation at normal temperature, high adsorption capacity, and good recycle potential of the new adsorbent would make it an ideal material for the removal of fluoride from drinking water.

Keywords: Fluoride; Orange peel; Zirconium; Adsorption; Kinetic; Isotherm

1. Introduction

Fluoride contamination of ground water is caused by natural and anthropogenic sources. The ubiquitous presence of fluoride in ground water has become a worldwide environmental issue because of its detrimental effects on human health. Excess of fluoride ingestion for a long time would lead to dental and skeletal fluorosis, bone disease, and nonskeletal fluorosis [1]. The problem of excess fluoride in drinking

water has engulfed in many parts of the world. According to WHO, fluorosis is endemic in at least 25 countries across the globe and has affected millions of people [2]. In India, 62 millions of people including 6 million children are suffering from fluorosis due to consumption of water having high fluoride concentration [3]. Hence, it becomes necessary to bring down the fluoride concentration within the permissible limit of 1.5 mg L^{-1} prescribed by WHO.

Many techniques of water defluoridation have been developed based on adsorption and biosorption [4–7], ion exchange [8], chemical precipitation [9,10],

*Corresponding author.

and membrane process, such as reverse osmosis [11], donnan dialysis [12], nanofiltration [13], and electro-dialysis [14]. Most of the observed methods are effective and can remove the fluoride to the permissible level, but the shortcomings of most of these methods are high operational and maintenance cost, secondary pollution (generation of toxic sludges), and complicated procedure involved in the treatment. Among these methods, adsorption is considered to be better as compared to other methods in terms of cost, simplicity of operation, and selectivity. Different adsorbents have been reported for the removal of fluoride from drinking water, such as activated alumina [15,16], metal oxides [17–23], carbon nanotubes [24], layered double hydroxides [25], and Mg/Al hydrotalcite [26,27]. The shortcomings of most of these materials are high cost, low fluoride adsorption capacity, and pH-dependent. So, the development of cheap and eco-friendly sorbent that would effectively remove the fluoride at neutral pH is, therefore, a challenging area of research and deserves immediate attention.

Since the operational cost of the adsorption process is dependent on the price of adsorbent, so there is a growing interest for using precursors (i.e. waste as an adsorbent). The natural occurrence of abundant amount of functional groups make various agricultural wastes a good alternative to expensive synthetic adsorbents prepared through complicated synthetic routes for the decontamination of various toxic chemicals [28]. Many low-cost adsorbents prepared from various wastes or generated from fisheries have been studied to remove the toxic ions from the aqueous solution. Some of the reported adsorbents include peanut hulls, wheat shell, apple residues, crab shell, rice husk, etc [29–34].

The bio-waste material investigated in this study is the orange peel (OP) generated from orange juice factories. Orange waste contains cellulose, hemicelluloses, lignin, and pectin. Pectin constitutes 10% of orange waste as an intracellular cementing material in its cell wall. Pectin is a polysaccharide that mainly consists of esterified D-galacturonic acid residing in alpha (1–4) chain. It essentially consists of hydroxyl and methyl ester groups. The ester and hydroxyl groups of pectin do not bind significantly with metals [35]. Hence, the present article reports the modification of OP by saponification of ester group with sodium hydroxide followed by the carboxylation of hydroxyl group with chloroacetic acid, thereby increasing the number of carboxylate ligands. The modified OP increases the zirconium binding ability of the biomass that can uptake fluoride from aqueous solution by ligand-exchange mechanism.

The prepared adsorbent material was characterized by FTIR, TGA/DTA, and XRD techniques. Surface morphology of the prepared material was studied using scanning electron micrography (SEM) coupled with energy-dispersive spectrum (EDS) technique. The textural properties of the synthesized material were determined by the N₂-BET method using a surface area porosimeter analyzer. The fluoride adsorption capacity of zirconium (IV)-loaded carboxylated orange peel (ZCOP) has been investigated in a batch mode. Batch adsorption studies were conducted under various experimental conditions such as pH, contact time, initial fluoride concentrations, temperature, and the presence of interfering ions. Attempts have also been made to understand the adsorption isotherm, kinetic, and mechanism of adsorption. The defluoridation capacity of the present adsorbent was also studied with the real ground water samples collected from endemic fluorosis area.

2. Materials and methods

2.1. Preparation of adsorbent

OP, zirconium oxychloride (Aldrich) and chloroacetic acid (Aldrich) were used for the synthesis of adsorbent. OP was collected from a fruit shop at BIT Mesra. OP was first cut into pieces, washed extensively with deionized water in order to remove water soluble organic compounds that may hinder the saponification process and was dried in an oven at 50°C until constant weight. The dried product was crushed and sieved to obtain smaller sized particles (OP). Hundred grams of washed OP was added to 0.1 M sodium hydroxide solution and was left for 24 h. It was then washed with deionized water until neutral pH and dried in an oven at 50°C to get saponified orange peel (SOP). Ten grams of SOP was added to 0.1 M chloroacetic acid solution, and 0.1 M sodium hydroxide was added dropwise to it until pH 8–10. It was aged for 24 h and was washed with deionized water until pH 7.0 and dried at 50°C yielding carboxylated orange peel (COP). Ten grams of COP was added to 0.1 M zirconium oxychloride solution. Then, the mixture was stirred for 24 h at a temperature of (25 ± 2)°C. After a time period of 24 h, the stirring process was stopped, but both the metal solution and carboxylated OP were allowed to remain in contact for further 48 h to ensure the maximum loading of zirconium on to the COP. After filtration, it was washed several times with distilled water followed by hot water in order to remove the free zirconium ions from the COP. The final product was dried at 60°C and thereafter named as ZCOP. The product was

crushed and sieved to obtain a particle size of 100–150 μm . The amount of zirconium loaded on COP was evaluated by measuring the zirconium concentration in the filtrate by ICPOES. The zirconium content in ZCOP was found to be 4.17 m mol g^{-1} which is higher than the SOJR-Zr which is 1.62 m mol g^{-1} as reported by Paudyal et al. 2012 [36].

2.2. Batch adsorption study

The removal of fluoride was tested in a batch process. Thus, 100 mL fluoride solution of desired concentration was taken into PVC conical flask to which known amount of adsorbent (ZCOP) was added. The entire mixture was shaken for 24 h using horizontal rotary shaker (shaking speed 200 rpm) to attain the equilibrium. Initial fluoride concentration was maintained at 10 mg L^{-1} for all the experiments except in those where the effects of initial fluoride concentration is to be studied. The residual concentration of fluoride in filtrate was determined using ion selective electrode. All adsorption experiments were carried out at room temperature (25 ± 2) $^{\circ}\text{C}$, except for the case where temperature variation is a parameter. The pH of the solution was adjusted using either HCl or NaOH. The effect of co-anions, such as chloride, sulfate, nitrate, bicarbonate, and phosphate, upon the adsorption process was studied by adding required amount of NaCl, Na_2SO_4 , NaNO_3 , NaHCO_3 , NaH_2PO_4 to a 100 mL of 10 mg L^{-1} fluoride solution. The concentration of fluoride on adsorbent was calculated using following equation:

$$q_e = (C_0 - C_e)(V/W) \times 100 \quad (1)$$

where q_e is the adsorption capacity (mg g^{-1}) in the solid at equilibrium; C_0 and C_e are initial and equilibrium concentrations of fluoride (mg L^{-1}), respectively; V is volume of the aqueous solution (L), and W is the mass (g) of adsorbent used in the experiments. The reusability of adsorbent material was checked by adding 0.7 g of adsorbent to 100 mL of 10 mg L^{-1} fluoride solution. The adsorbent was filtered and dried in an oven at 50°C in vacuum. Subsequently, the dried adsorbent material was used repeatedly for fluoride removal in various samples to determine the extent of adsorption. Each experiment was carried out in duplicate, and the average results were presented in the work.

2.3. Analytical measurements

The FTIR spectra of all the sample materials were recorded at room temperature at a resolution of

4 cm^{-1} and 64 scans using Shimadzu IR Prestige-21 FTIR instrument. SEM of the sample was obtained in a JSM 6390 LV apparatus coupled with EDS. The X-ray diffraction pattern was obtained on a Shimadzu model XD3A diffractometer (40 kV/30 mA), in the range of $2\theta = 1.5\text{--}70^{\circ}$ with a nickel-filtered Cu $K\alpha$ radiation, at wavelength of 1.54 \AA . BET surface area measurement was taken using Quantachrome automated gas sorption system. The Thermogravimetric analysis (TGA/DTA) was carried out using Shimadzu DTG 60 in nitrogen atmosphere under a flow of 30 mL min^{-1} and heating rate of $10^{\circ}\text{C min}^{-1}$ varying the temperature from 25 to 1,000 $^{\circ}\text{C}$. The metal ion concentration was determined by Perkin–Elmer, Optima 2100 DV, ICPOES. Concentration of fluoride in the solution, before and after adsorption, was determined using ion selective electrode (Orion 720 A + Ion analyzer). The metal ion concentration was determined by Perkin–Elmer Optical 2100DV, ICPOES.

3. Results and discussion

3.1. Adsorbent characterization

3.1.1. Infrared

The FTIR spectrum of the adsorbent material was recorded and was analyzed for the detection of surface functional groups on adsorbent. The FTIR spectrum of the prepared zirconium-impregnated modified orange peel (ZCOP) and fluoride adsorbed ZCOP (FZCOP) is shown in Fig. 1. In the spectra of ZCOP, a broad peak around 3,569 cm^{-1} shows the presence of surface –OH groups. A peak at 496 cm^{-1} in ZCOP indicating the presence of Zr–O bond [37]. Also, the peak at 3,569 cm^{-1} in case of ZCOP shifts to 3,615 cm^{-1} showing the participation of hydroxyl anion in ligand exchange with the fluoride ion.

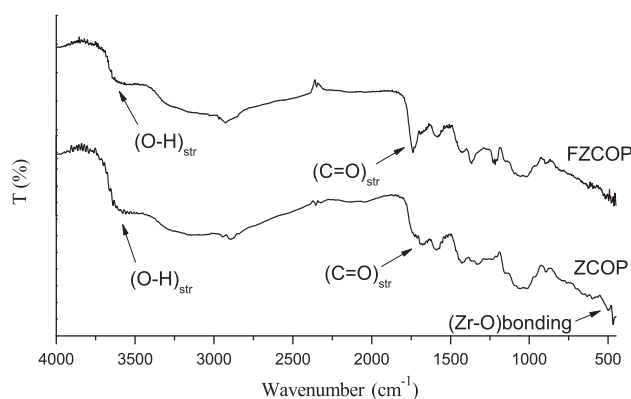


Fig. 1. FTIR spectrum of ZCOP and FZCOP.

3.1.2. Thermogravimetric analysis

TGA is an important way to determine the thermal stability of a material. The TGA-DTA curves of both COP and ZCOP in the range of 25–1,000°C are shown in Fig. 2(a) and (b). The weight loss observed in the range of 25–185°C and the corresponding endothermic peak in the DTA curve can be attributed to the evaporation of chemically and physically adsorbed water molecules and other volatile chemicals. The degradation of pectin, hemicellulose, and cellulose could be concluded by the weight loss in the range 185–300°C. The weight loss observed in the range of 300–550°C is due to the degradation of lignin. In case of COP, the total weight loss observed was 99.71%, while the total weight loss occurred in case of ZCOP was 97.21% within the range of study which showed a total of 2.79% of metallic residue due to the impregnation of zirconium on COP.

3.1.3. Scanning electron micrography

The scanning electron micrographs of the ZCOP and FZCOP are shown in Fig. 3(a) and (b). The corresponding EDS spectrum is also embedded on the micrographs. The adsorption of fluoride on ZCOP can be concluded by the presence of whitish spots distributed all over the material as shown in the micrograph of FZCOP which is further confirmed by its EDS spectrum.

3.1.4. X-ray diffractometry and surface area determination

Fig. 4 shows the XRD pattern of the prepared material. The result is compared with similar kind of

research work published by Kobayashi et al. [38]. The composite material indicated the presence of $\text{Zr}(\text{OH})_4$ and polymerized species. It is indicated that the loaded $\text{Zr}(\text{OH})_4$ is transformed to an amorphous phase composed of polymerized species by incorporating water molecules. The specific surface area, micropore volume and average micropore diameter of ZCOP were determined to be $20.56 \text{ m}^2 \text{ g}^{-1}$, $0.0001 \text{ cm}^3 \text{ g}^{-1}$, and 2.62 nm, respectively.

3.2. Sorption studies

3.2.1. Effect of variation of adsorbent dose

The effect of variation of adsorbent dose on fluoride removal was studied by varying the dose from 0.2 to 1.2 g at a temperature of $(25 \pm 2)^\circ\text{C}$ with contact time period of 60 min and initial fluoride concentration of 10 mg L^{-1} . It was observed that with increase in adsorbent dose, fluoride adsorption increased which can be attributed to availability of more adsorption sites. The percentage of maximum fluoride removal was found to be 97.2% with an adsorbent dose of 0.7 g L^{-1} and further increase in adsorbent dose showed no quantitative effect upon adsorption. It is to be noted that no such adsorption was observed for raw OP.

3.2.2. Effect of variation of pH

The pH of solution strongly affects the sorption ability of any adsorbent material. The adsorption of fluoride onto ZCOP was studied at a pH range of 2–12. The graphical representation given in Fig. 5

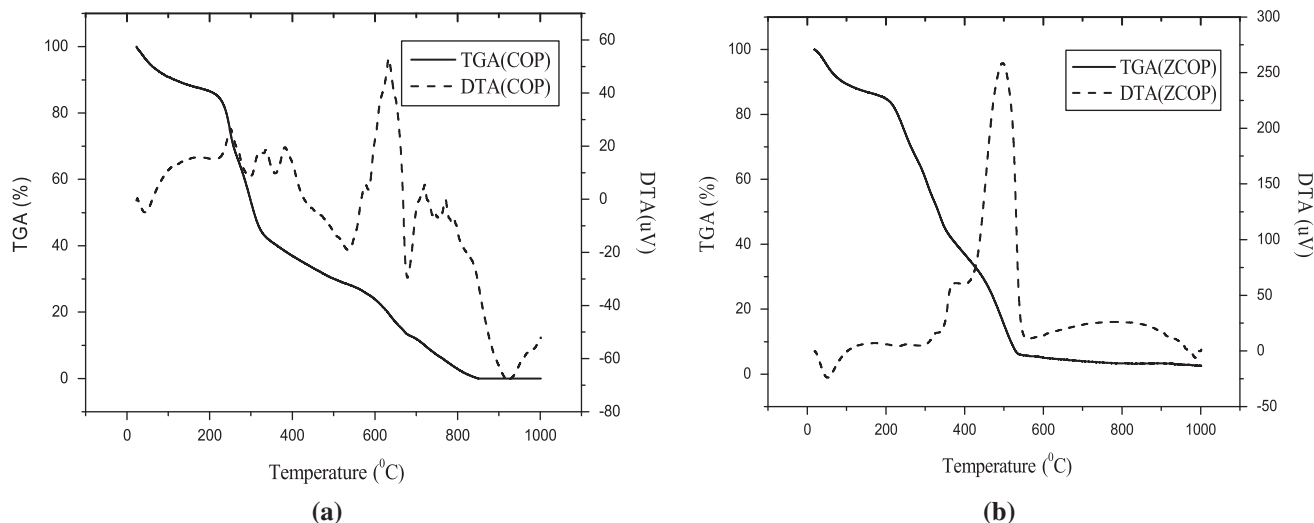


Fig. 2. TGA curve of COP and ZCOP.

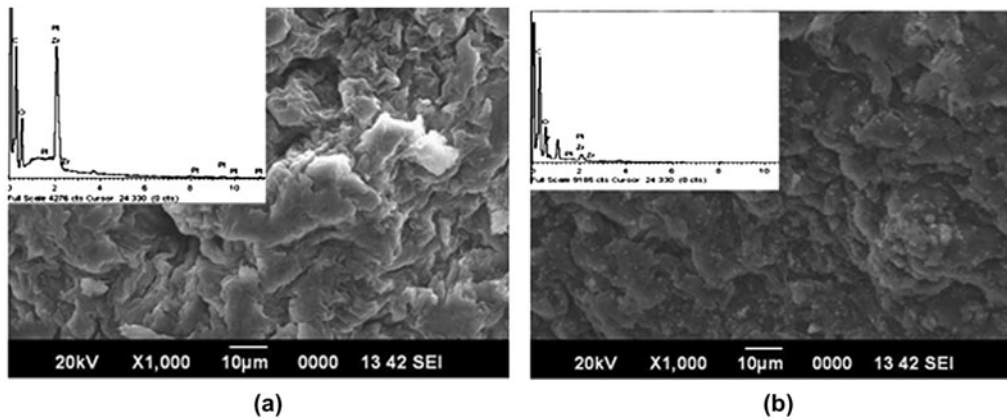


Fig. 3. SEM (embedded with EDS) of ZCOP and FZCOP.

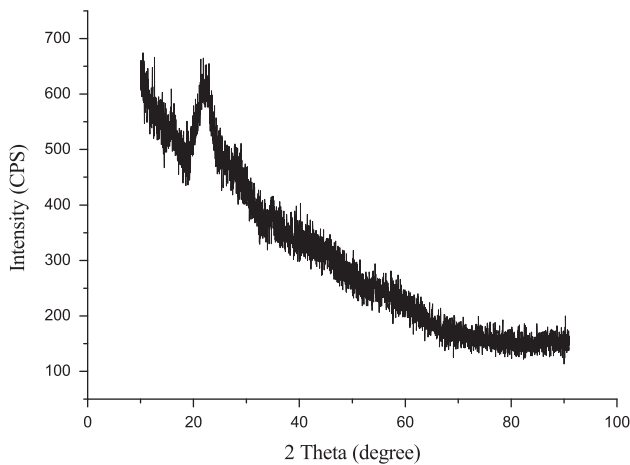


Fig. 4. X-ray diffractogram of ZCOP.

clearly shows that the adsorption by ZCOP increases as the pH increases showing 90% removal at pH 2 and 95–97% removal at a pH range 5–7. Adsorption of F^- at lower pH can be attributed to the electrostatic force of attraction provided by the positively charged surface of ZCOP and ligand exchange at neutral pH. However, at lower pH, the H^+ ions present in solution binds with the F^- ions to form HF due to which F^- ions are less available which accounts for lesser F^- adsorption at lower pH when compared to neutral pH. As the pH increases, the adsorption potential decreases which may be due to strong competition between hydroxyl and fluoride ions in solution.

3.2.3. Effect of variation of contact time period

The effect of variation of contact time period was studied at an initial fluoride concentration of 10 mg L^{-1}

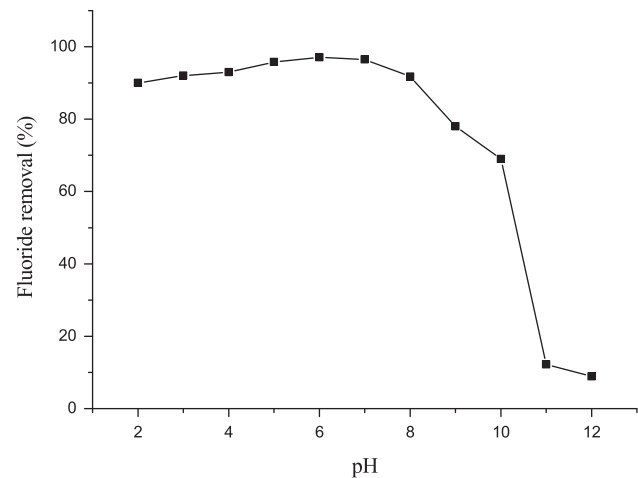


Fig. 5. Effect of pH on extent of removal of fluoride, conc. of fluoride: 10 mg L^{-1} ; time of contact: 60 min; adsorbent dose: 7.0 g/L (average value of two tests, error < 5%).

and increase in fluoride adsorption was observed with increase in contact time as shown in Fig. 6(a). Equilibrium was observed at a time period of 50 min accounting 97% fluoride removal after which no further removal was observed. This may be due to the fact that initially all adsorbent sites were available for anions and the initial solute concentration gradient was also high.

In order to interpret the experimental data, the time-dependent sorption data have been analyzed using three kinetic models: pseudo-first-order, pseudo-second-order, and intraparticle diffusion model. The mathematical representations of these models are given in Eqs. (2)–(4) [39].

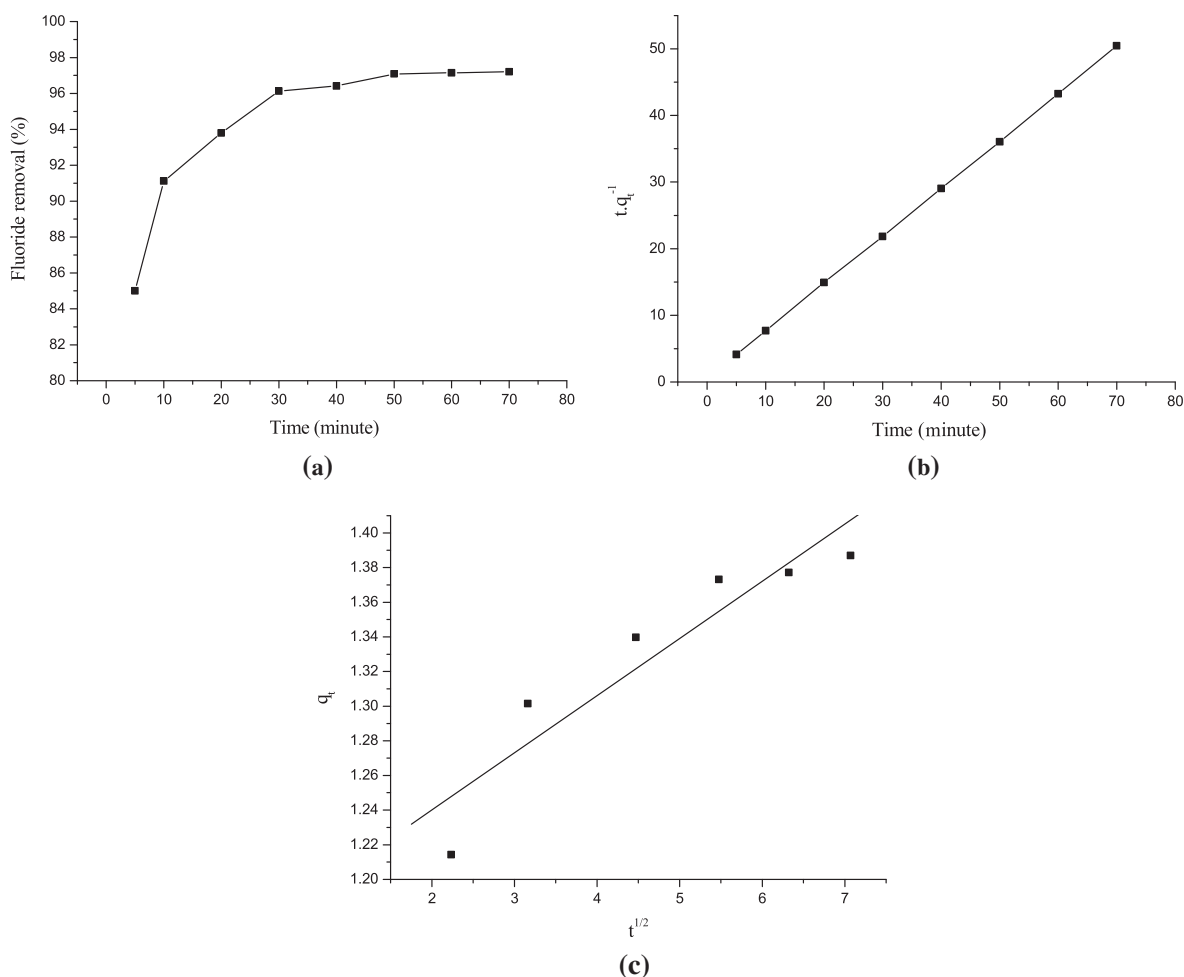


Fig. 6. Effect of contact time (a) Pseudo-second-order kinetic plot (b) and Weber–Morris intra-particle diffusion plot (c) for fluoride adsorption on ZCOP; conc. of fluoride: 10 mg L⁻¹; adsorbent dose: 7.0 g/L; pH: 6.0 (average values of two tests, error < 5%).

Pseudo-first-order model:

$$\log(q_e - q_t) = \log q_e - K_f t / 2.303 \quad (2)$$

where q_e and q_t denote the amount of fluoride adsorbed (mg g⁻¹) at equilibrium and at time t , respectively. K_f (min⁻¹) is the rate constant of pseudo-first-order adsorption reaction.

Pseudo-second-order model: $t/q_t = 1/K_s(q_e)^2 + t/q_e$ (3)

where K_s is the rate constant for the pseudo-second-order reaction (g mg⁻¹ min⁻¹). q_e and q_t are the amounts of solute sorbed at equilibrium and at any time t (mg g⁻¹), respectively.

The intraparticle diffusion model: $q_t = K_i t^{1/2} + C$ (4)

where K_i is the intraparticle diffusion constant (mg g⁻¹ min^{-1/2}), and C is the intercept. The rate constants and other parameters obtained from the graphs of the kinetic models (Fig. 6(b) and (c)) are presented in Table 1.

Analyzing the data, it can be concluded that the adsorption of fluoride on to ZCOP follow pseudo-second-order model for which the value of correlation coefficient (R^2) is found to be 1 and the values of q_{erexp} and q_{ercal} are also found to be very close to each other. From the Weber–Morris intraparticle diffusion plot, the value of intercept C provides information about the thickness of boundary layer, that is, the resistance to the external mass transfer. The larger is the value of the intercept, and the higher is the external resistant. The deviation of straight line from the origin, as shown in Fig. 6(c),

Table 1

Kinetic parameters for fluoride adsorption onto ZCOP at pH 6.0; adsorbent dose: 7.0 g L⁻¹ temp: 298 K, initial fluoride conc. 10 mg L⁻¹

Pseudo-first order*				Pseudo-second order*				Intra-particle diffusion*		
q _{exp}	K _f	q _{e,cal}	R ²	K _s	h	q _{e,cal}	R ²	K _i	C	R ²
1.387	0.0833	0.226	0.969	0.886	1.751	1.405	1.0	0.033	1.1741	0.8713

*The units for q_{exp}, q_{e,cal}: mg g⁻¹; K_f: L min⁻¹; K_s, h: (mg g⁻¹ min⁻¹); K_B: min⁻¹; K_i, C: mg. (g min^{1/2})⁻¹

may be due to the difference between the rate of mass transfer in the initial and final stages of adsorption, which indicates that the pore diffusion is not the sole rate-controlling step.

3.2.4. Effect of variation of initial fluoride concentration

The relationship between the initial fluoride concentration and adsorption was investigated by varying the fluoride concentration within the range of 2–100 mg L⁻¹. For this experiment, a contact time period of 50 min, an adsorbent dose of 0.7 g L⁻¹ and solution volume of 100 mL was maintained. A decreasing behavior of fluoride removal was observed with increase in fluoride concentration. It may be due to the fact that with increase in concentration of fluoride in solution, the available co-ordination sites get saturated, thereby reflecting a decreased trend of binding ability of adsorbent. With the lowest initial fluoride concentration, the removal of fluoride was almost 98.5% which reduced to 67% at initial concentration of 100 mg L⁻¹. To quantify the adsorption capacity of ZCOP, four isotherm models, that is, Langmuir, Freundlich, Temkin, and D–R model have been adopted. Langmuir isotherm model is based on the monolayer adsorption on a structurally homogeneous surface, whereas Freundlich isotherm model is based on the multilayer adsorption of an adsorbate on to the heterogeneous adsorbent surface. Temkin isotherm model is based on the adsorbent/adsorbate interactions that are linear in nature and the adsorption is characterized by uniform distribution of binding energies. D–R isotherm is used to find out the free energy of adsorption and hence the adsorption mechanism. These models are represented mathematically as follows [40]:

$$\text{Langmuir isotherm: } 1/q_e = (1/K_L q_m)(1/C_e) + 1/q_m \quad (5)$$

where C_e (mg L⁻¹) is the concentration of fluoride at equilibrium, K_L (L mg⁻¹) and q_m (mg g⁻¹) are the Langmuir constants related to the energy of

adsorption and maximum adsorption capacity, respectively.

$$\text{Freundlich isotherm: } \ln q_e = \ln K_F + 1/n \ln C_e \quad (6)$$

where K_F (mg^{1 - (1/n)} L^{1/n} g⁻¹) and 1/n are the Freundlich constants related to adsorption capacity and intensity, respectively.

$$\text{Temkin isotherm: } q_e = B_1 \ln A + B_1 \ln C_e \quad (7)$$

where A is the equilibrium binding constant (L mol⁻¹) corresponding to the maximum binding energy, and the constant B₁ is related to the heat of adsorption.

$$\text{D–R isotherm: } \ln q_e = \ln q_m - K \varepsilon^2 \quad (8)$$

where ε² is the Polanyi potential which is equal to RT ln(1 + 1/C_e). q_e is the amount of adsorbate adsorbed at equilibrium per unit of adsorbent (g g⁻¹), q_m is the theoretical saturation capacity (g g⁻¹), C_e is the equilibrium solid concentration (g L⁻¹). K is the constant related to adsorption energy and gives the value of mean free energy of adsorption. R is the gas constant and T is the temperature in Kelvin.

In order to understand the mechanism of fluoride adsorption onto ZCOP, the experimental data was subjected to Langmuir, Freundlich, Temkin, and D–R isotherm models. The experimental data on adsorption isotherm together with the predicted Langmuir, Freundlich, Temkin, and D–R isotherm simulation curves are presented in Fig. 7 and corresponding values are presented in Table 2.

Optimization of regression analysis data was done using six different six different error functions, that is, the sum of square of errors (SSE), the sum of absolute errors (SAE), the average relative errors (ARE), the hybrid fractional errors (HYBRID), the Marquardt's percent standard deviation (MPSD), and relative standard deviation (R²). The computational

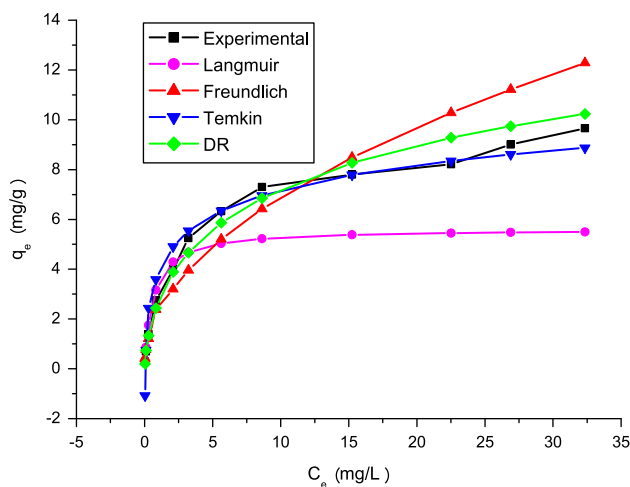


Fig. 7. Adsorption isotherm modeling of fluoride removal by ZCOP using linear regression analysis; adsorbent dose: 7.0 g/L; pH 6.0, temp (25 ± 2)°C; contact time: 50 min.

Table 2
Linear Freundlich, Langmuir, Temkin, and D–R isotherm constants related to the sorption of fluoride onto ZCOP

Model/parameters	Linear method
Freundlich	
K_F	2.226
$1/n$	0.491
Langmuir	
K_L	1.555
q_m	5.605
Temkin	
b	1715.889
A	14.425
D–R	
q_m	0.015
K	0.0061

result of all six different error functions are presented in Table 3 which indicated that D–R isotherm model is the most suitable model to satisfactorily describe the adsorption phenomenon based on the highest R^2 value and lowest SSE, SAE, ARE, HYBRID, and MPSD values.

3.2.5. Effect of variation of temperature

The spontaneity of the adsorption process was predicted by observing the effect of change of temperature upon adsorption and hence calculating the various thermodynamic parameters. The temperature was varied from 10 to 50°C. It was observed that with

increase in temperature, fluoride adsorption increased which may be attributed to the fact that adsorption is endothermic in nature. The feasibility of the process can be determined by calculating the value of ΔG° which is given by the Vant Hoff equation:

$$\Delta G^\circ = -RT \ln K_D \quad (9)$$

where ΔG° is the change in free energy, T is the absolute temperature, R is the universal gas constant (8.314 J mol⁻¹ K⁻¹), and K_D is the equilibrium constant. Negative values of ΔG° as shown in the Table 4 indicate the spontaneity of the adsorption process. With increase in temperature, ΔG° values increases showing the increase in spontaneity. The values of ΔH° and ΔS° associated with the process can be calculated by the equation:

$$\ln K_D = \Delta S^\circ / R - \Delta H^\circ / RT \quad (10)$$

Values of ΔH° and ΔS° can be obtained from the straight line equation of the plot between $\ln K_D$ and $1/T$ Fig. 8. Endothermic nature of the adsorption process can be concluded by the positive value of ΔH° . Sticking probability (S^*) was further computed which is related to the surface coverage (θ) by the adsorbed molecule and associated activation energy.

$$S^* = (1 - \theta) \exp(-E_a/RT) \quad (11)$$

where θ gives the surface coverage which is given by

$$\theta = 1 - C_e/C_0 \quad (12)$$

where C_0 and C_e represent the initial and equilibrium fluoride ion concentrations, respectively. Both values of E_a and θ can be calculated, respectively, from the slope and intercept of the plot of $\ln(1 - \theta)$ vs. $1/T$. The positive values of ΔH° and activation energy E_a confirm the endothermic nature of the sorption process. The value of S^* is found to be 0, clearly indicating that the adsorption follows a chemisorption process.

3.2.6. Mechanism

The proposed mechanism of fluoride adsorption and desorption by ZCOP is presented in Fig. 9. The fluoride removal by ZCOP could be due to the exchange between the water coordinated with the adsorbent and fluoride which is similar to adsorption of arsenic on zirconium(IV) loaded orange waste gel and antimony on Fe(III) loaded gel [41,42]. The use of zirconium ion, in particular, preferred as a material of choice due to the fact that the tetravalent zirconium

Table 3
Isotherm error deviation data related to the sorption of fluoride onto ZCOP using six commonly used functions

Error functions	R^2	SSE	SAE	ARE	HYBRID	MPSD
Linear approach						
Freundlich	0.956	21.038	12.416	20.361	24.433	25.022
Langmuir	0.988	50.097	18.102	23.453	28.144	28.92
Temkin	0.959	5.541	6.232	53.657	64.388	154.69
D–R	0.994	3.103	4.919	9.187	11.024	12.395

Table 4
Thermodynamic parameters for the sorption of fluoride on ZCOP

Temp (°C)	ΔH° (kJ mol ⁻¹)	ΔS° (kJ mol ⁻¹ K ⁻¹)	ΔG° (kJ mol ⁻¹)	E_a (kJ mol ⁻¹)	S^*
10	41.111	0.206	-17.413	39.69	0
20			-19.481		
30			-21.549		
40			-23.617		
50			-25.685		

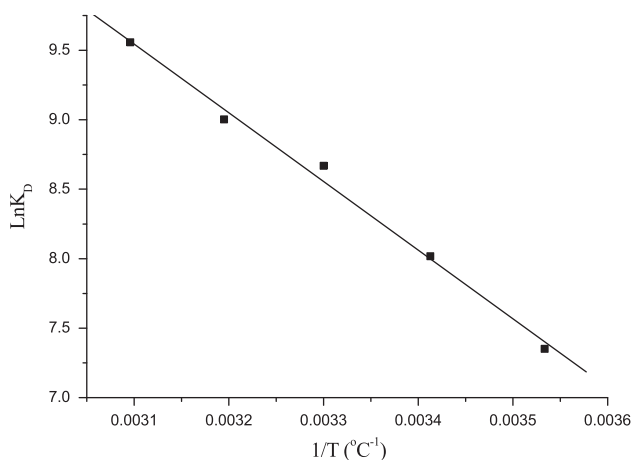


Fig. 8. Plot of $\log_{10} K_D$ vs. $1/T$ for ZCOP.

in its hydrated form can generate tetranuclear ions as well as octanuclear species with abundant hydroxyl ions and water molecules that can take part in ligand substitution reactions with fluoride ion [43]. Further, the hydroxyl ion and water molecule that may be available in the coordination sphere could also be contributing to the ligand-exchange reactions with fluoride ion [36]. Thus, a comparative feature of fluoride removal capacity of some commercially available sorbents with ZCOP is presented in Table 5. In comparison, ZCOP, which shows a higher defluoridation capacity, confirms its selectivity toward fluoride removal.

3.2.7. Effect of coexisting ions

Drinking water may contain several other ions such as sulfate, chloride, and nitrate, along with fluoride, which may compete with fluoride for active sorption sites. Therefore, the effect of various diverse ions/competing co-ions upon adsorption of fluoride was also investigated using the experimental condition for initial fluoride concentration at 10 mg L⁻¹, while varying the initial concentration of co-ions (chloride, sulfate, nitrate, bicarbonate, and phosphates) from 0 to 600 mg L⁻¹. The result of the observation for the effect of co-ions is shown graphically in Fig. 10 which indicates that NO₃⁻, Cl⁻, SO₄²⁻ had little effect upon fluoride removal processes, whereas the presence of both PO₄³⁺ and HCO₃⁻ reduces the fluoride uptake to almost 65–70% at an initial fluoride concentration of 600 mg L⁻¹. Hence, it is recommended to use other treatment processes that can be helpful in removal of both phosphate and bicarbonate prior to the removal of fluoride. The defluoridation efficiency of adsorbent was tested with the ground water sample collected from Odisha, India. A comparison between fluoride removal by the prepared adsorbent in case of synthetic water and collected ground water is presented graphically in Fig. 11. The synthetic water samples were prepared by adding sodium fluoride to de-ionized water. More fluoride removal was observed in case of synthetic water samples as compared to the collected ground water samples. The presence of large number of cations and anions in ground water could

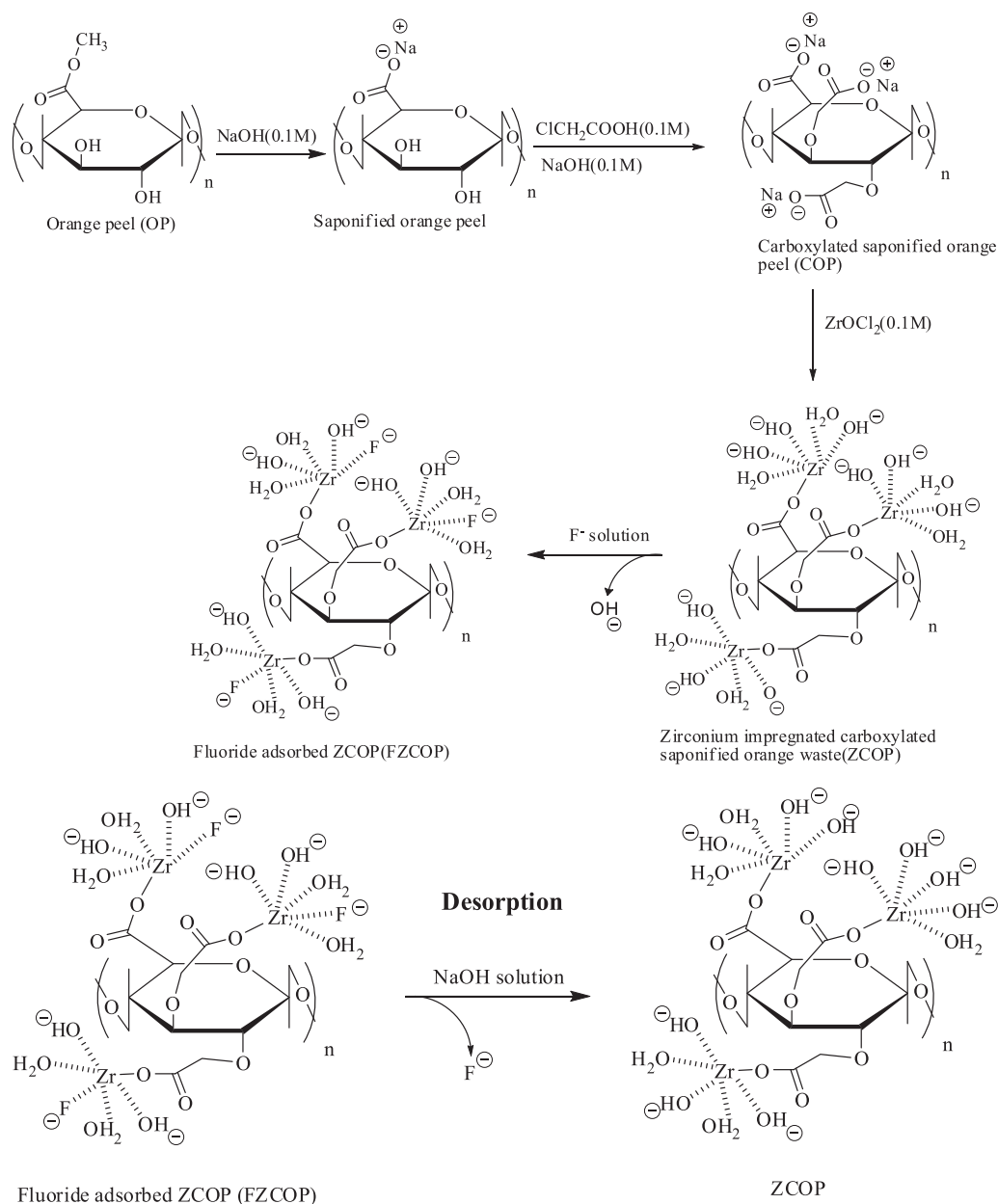


Fig. 9. Chemical modification of peel waste and proposed mechanism of adsorption/desorption of fluoride.

be the most probable reason for this since they could interfere with the adsorption process.

3.2.8. Reuse and regeneration

Effective reuse of adsorbent material directly affects the cost factor, and hence, its utility in continuous batch adsorption process. Only the adsorbent

material that can be reused have practical value in real systems. The test of reusable capacity of ZCOW was performed with dried ZCOW. The percentage of adsorption of fluoride by ZCOW was found to be reduced from 97 to 83% following a sequence of 1st to 8th cycle of operation Fig. 12. Desorption studies were carried out with different strengths of NaOH solutions. It was observed that at low concentration of NaOH (0.001 M), leaching of fluoride from adsorbent

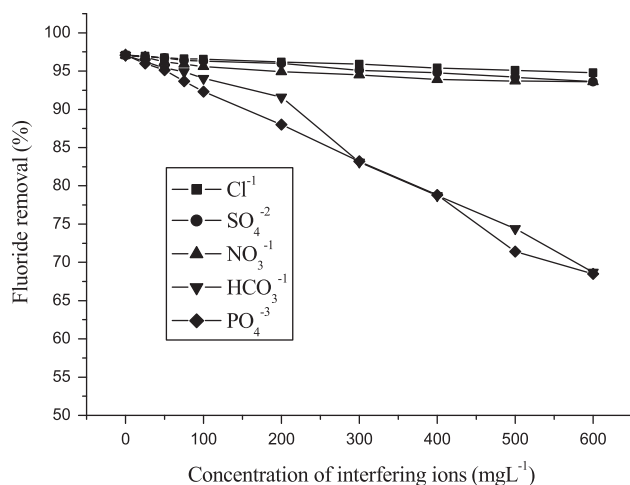


Fig. 10. Effect of co-ions upon removal of fluoride from solution; amount of adsorbent: 7.0 g/L; concentration of fluoride: 10 mg L⁻¹; time of contact: 50 min; temperature: (25 ± 2) °C.

was only 4%. However, with increased concentration of NaOH (0.1 M), leaching of fluoride from adsorbent reaches to 91%. Thus, it can be concluded that the

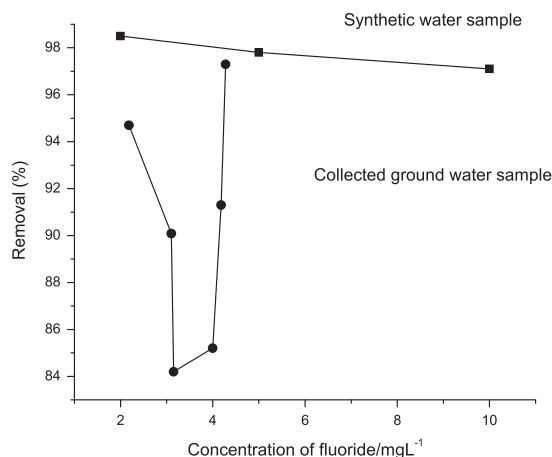


Fig. 11. Comparison of adsorption of fluoride in synthetic water and collected ground water sample; amount of adsorbent: 7.0 g/L; time of contact: 50 min; temperature: (25 ± 2) °C.

prepared adsorbent ZCOP can be regenerated and used for several cycles of operations.

Table 5

Comparative assessment of adsorption capacity of zirconium loaded carboxylated orange peel (ZCOP) with some literature available data

Adsorbent	q_m mg/g	Experimental conditions	Reference
Manganese oxide coated alumina	2.85	pH: 7.0 C_0 : 2.5–30	[44]
Montmorillonite	3.365	pH: 6.0 C_0 : 2–120	[45]
Zr(IV) impregnated collagen fibre	2.18	pH: 5.5 C_0 : 19–95	[46]
Activated alumina	2.41	pH: 7.0 C_0 : 2.5–14	[16]
Aluminum impregnated activated alumina	1.07	pH: 3 C_0 : 0.5–15	[6]
Aluminum-amberlite resin	4.6	pH: 4.0 C_0 : 4–9.1	[47]
La(III) impregnated carboxylated chitosan	4.711	pH: 7.0 C_0 : 11–19	[48]
Protonated chitosan beads	1.664	pH: 7.0 C_0 : 11–19	[49]
Boehmite	2.057	pH: 4.5–7.5 C_0 : 5–50	[50]
MnO ₂ coated tamarind fruit	1.99	pH: 6.5 C_0 : 2–5	[51]
ZCOP	5.605	pH: 6.0 C_0 : 2–50 mg L ⁻¹	Present work

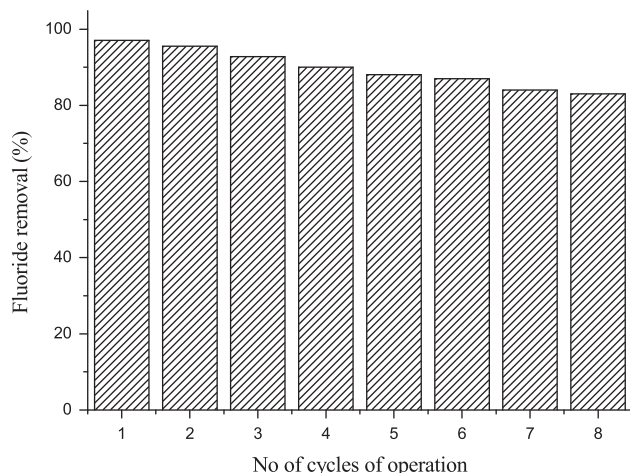


Fig. 12. Percentage of removal of fluoride by ZCOP in different cycles of batch operation.

4. Conclusion

This study reports the formation of a new adsorbent zirconium-impregnated modified orange waste (ZCOP) which was used for the removal of fluoride from ground water. The conclusions of the study are reported below:

- (1) Maximum fluoride removal could be achieved at an adsorbent dose of 0.7 g L^{-1} at neutral pH which shows that the adsorbent can be used directly with the sample water at its natural pH without any pre-treatment.
- (2) The adsorption process followed a pseudo-second-order kinetic model. By the analysis of the compiled data of the error functions, it can be concluded that the D-R isotherm model is the most suitable model to satisfactorily describe the studied adsorption phenomenon based on the highest R^2 value and lowest SSE, SAE, ARE, HYBRID, and MPSD values.
- (3) The value of E was found to be $9.0535 \text{ kJ mol}^{-1}$ suggesting that the adsorption proceeds by ion-exchange process. The value of ΔG° at all temperatures was negative showing the spontaneity of the adsorption process. Further, the positive value of ΔH° confirms the endothermic nature of the process. The value of ΔS° was $0.206 \text{ kJ mol}^{-1} \text{ K}^{-1}$ indicating a relatively ordered state rather than a chaotic distribution.
- (4) The presence of co-anions in the water sample such as NO_3^- , Cl^- , SO_4^{2-} had no effect on the removal of fluoride. However, the presence of HCO_3^- and PO_4^{3-} reduced the efficiency of adsorbent for selective fluoride removal.

- (5) The adsorbent can be regenerated and hence can be reused up to 8th cycle which makes it a potential adsorbent for the removal of fluoride.

Acknowledgment

The analytical facilities provided by Central Instrumentation Facility, BIT, Mesra is thankfully acknowledged.

References

- [1] D.P. Das, J. Das, K. Parida, Physicochemical characterization and adsorption behaviour of calcined Zn/Al hydrotalcite-like compound (HTlc) towards removal of fluoride from aqueous solution, *J. Colloid Interface Sci.* 261 (2003) 213–220.
- [2] World Health Organisation, 20 avenue appia, 1211 Geneva 27, Switzerland, Guidelines for Drinking-water Quality: Incorporating First Addendum Recommendations, 1st, 3rd ed., 2006, pp. 375–376.
- [3] A.K. Susheela, Fluorosis management programme in India, *Curr. Sci.* 77 (1999) 1250–1256.
- [4] X. Wu, Y. Zhang, X. Dou, M. Yang, Fluoride removal performance of a novel Fe–Al–Ce trimetal oxide adsorbent, *Chemosphere* 69 (2007) 1758–1764.
- [5] S. Ayoob, A.K. Gupta, Sorptive response profile of an adsorbent in the defluoridation of drinking water, *Chem. Eng. J.* 133 (2007) 273–281.
- [6] S.S. Tripathy, J. Bersillon, K. Gopal, Removal of fluoride from drinking water by adsorption onto alum-impregnated activated alumina, *Sep. Purif. Technol.* 50 (2006) 310–317.
- [7] L. Chen, B. He, S. He, T. Wang, C. Su, Y. Jin, Fe–Ti oxide nano-adsorbent synthesized by co-precipitation for fluoride removal from drinking water and its adsorption mechanism, *Powder Technol.* 227 (2012) 3–8.
- [8] S. Meenakshi, N. Viswanathan, Identification of selective ion-exchange resin for fluoride sorption, *J. Colloid Interface Sci.* 308 (2007) 438–450.
- [9] G. Chae, S. Yun, B. Mayer, K. Kim, S. Kim, J. Kwon, K. Kim, Y. Koh, Fluorine geochemistry in bedrock groundwater of South Korea, *Sci. Total Environ.* 385 (2007) 272–283.
- [10] J. Zhu, H. Zhao, J. Ni, Fluoride distribution in electrocoagulation defluoridation process, *Sep. Purif. Technol.* 56 (2007) 184–191.
- [11] R. Simons, Trace element removal from ash dam waters by nanofiltration and diffusion dialysis, *Desalination* 89 (1993) 325–341.
- [12] E. Kir, E. Alkan, Fluoride removal by Donnan dialysis with plasma-modified and unmodified anion-exchange membranes, *Desalination* 197 (2006) 217–224.
- [13] M. Tahaikt, R. El Habbani, A.A. Haddou, I. Achary, Z. Amor, M. Taky, A. Alamib, A. Boughriba, M. Hafsi, A. Elmidaou, Fluoride removal from groundwater by nanofiltration, *Desalination* 212 (2007) 46–53.
- [14] M. Tahaikt, I. Achary, M.A. Menkouchi Sahli, Z. Amor, M. Taky, A. Alami, M. Boughriba, M. Hafsi,

- A. Elmidaoui, Defluoridation of Moroccan ground water by electrodialysis, *Desalination* 167 (2004) 357–365.
- [15] S. Ghorai, K.K. Pant, Equilibrium, kinetics and breakthrough studies for adsorption of fluoride on activated alumina, *Sep. Purif. Technol.* 42 (2005) 265–271.
- [16] Y. Ku, H. Chiou, The adsorption of fluoride ion from aqueous solution by activated alumina, *Water Air Soil Pollut.* 133 (2001) 349–360.
- [17] B. Nagappa, G.T. Chandrappa, Mesoporous nanocrystalline magnesium oxide for environmental remediation, *Micropor. Mesopor. Mater.* 106 (2007) 212–218.
- [18] D. Mohapatra, D. Mishra, S.P. Mishra, G.R. Chaudhary, R.P. Das, Use of oxide minerals to abate fluoride from water, *J. Colloid Interface Sci.* 275 (2004) 355–359.
- [19] Z. Li, S. Deng, X. Zhang, W. Zhao, J. Huang, G. Yu, Removal of fluoride from water using titanium-based adsorbents, *Front. Environ. Sci. Eng. Chin.* 4 (2010) 414–420.
- [20] K. Babaeiveli, A.P. Khodadoust, Adsorption of fluoride onto crystalline titanium dioxide: Effect of pH, ionic strength, and co-existing ions, *J. Colloid Interface Sci.* 394 (2013) 419–427.
- [21] J. Lu, H. Liu, R. Liu, X. Zhao, L. Sun, J. Qu, Adsorptive removal of phosphate by a nanostructured Fe–Al–Mn trimetal oxide adsorbent, *Powder Technol.* 233 (2013) 146–154.
- [22] X. Dou, D. Mohan, C.U. Pittman Jr., S. Yang, Remediating fluoride from water using hydrous zirconium oxide, *Chem. Eng. J.* 198–199 (2012) 236–245.
- [23] J.P. Nordin, D.J. Sullivan, B.L. Phillips, W.H. Casey, Mechanisms for fluoride promoted dissolution of bayerite [β -Al(OH)₃(S)] and boehmite [γ -AlOOH]: ¹⁹F-NMR spectroscopy and aqueous surface chemistry, *Geochim. Cosmochim. Acta* 63(21) (1999) 3513–3524.
- [24] Y.H. Li, S. Wang, X. Zhang, J. Wei, C. Xu, Z. Luan, D. Wu, Adsorption of fluoride from water by aligned carbon nanotubes, *Mater. Res. Bull.* 38 (2003) 469–476.
- [25] L. Liang, J. He, M. Wei, X. Duan, Kinetic studies on fluoride removal by calcined layered double hydroxides, *Ind. Eng. Chem. Res.* 45 (2006) 8623–8628.
- [26] H. Wang, J. Chena, Y. Caia, J. Jia, L. Liua, H. Teng, Defluoridation of drinking water by Mg/Al hydrotalcite-like compounds and their calcined products, *Appl. Clay Sci.* 35 (2007) 59–66.
- [27] K. Hosni, E. Srasra, Evaluation of fluoride removal from water by hydrocalcite-like compounds synthesized from the kaolinic clay, *J. Water Chem. Technol.* 33 (2010) 164–176.
- [28] H. Hasar, Adsorption of Nickel(II) from aqueous solution onto activated carbon prepared from almond husk, *J. Hazard. Mater.* 97 (2003) 49–57.
- [29] P. Brown, I.A. Jefcoat, D. Parrish, S. Gill, E. Graham, Evaluation of adsorptive capacity of peanut hull pellets for heavy metals in solution, *Adv. Environ. Res.* 4 (2000) 19–29.
- [30] K.K. Singh, M. Talat, S.H. Hasan, Removal of lead from aqueous solutions by agricultural waste maize bran, *Bioresour. Technol.* 97 (2006) 2124–2130.
- [31] U. Kumar, M. Bandyopahyay, Sorption of Cadmium from aqueous solution using pretreated rice husk, *Bioresour. Technol.* 97 (2006) 104–109.
- [32] Y. Orhan, H. Buyukgungor, The removal of heavy metals by using agricultural wastes, *Water Sci. Technol.* 28 (1993) 247–255.
- [33] A.K. Yadav, R. Abbassi, A. Gupta, M. Dadashzadeh, Removal of fluoride from aqueous solution and groundwater by wheat straw, sawdust and activated bagasse carbon of sugarcane, *Ecol. Eng.* 52 (2013) 211–218.
- [34] M. Ghorbani, H. Eisazadeh, Removal of COD, color, anions and heavy metals from cotton textile wastewater by using polyaniline and polypyrrole nanocomposites coated on rice husk ash, *Composites Part B* 45 (2013) 1–7.
- [35] F. Ning-chuan, G. Xue-yi, L. Sha, Enhanced Cu(II) adsorption by orange peel modified with sodium hydroxide, *Trans. Nonferrous Met. Soc.* 20 (2010) 146–152.
- [36] H. Paudyal, B. Pangen, I. Katsutoshi, M. Miyuki, R. Suzuki, H. Kawakita, K. Ohto, B.K. Biswas, S. Alam, Adsorption behaviour of fluoride ions on zirconium(IV)-loaded orange waste gel from aqueous solution, *Sep. Sci. Technol.* 47 (2012) 96–103.
- [37] Y. Zheng, S. Lim, J.P. Chen, Preparation and characterization of zirconium-based magnetic sorbent for arsenate removal, *J. Colloid Interface Sci.* 338 (2009) 22–29.
- [38] T. Kobayashi, T. Sasaki, Solubility of zirconium (IV) hydrous oxides, *J. Nucl. Sci. Technol.* 44 (2007) 90–94.
- [39] S.K. Swain, S. Mishra, T. Pattnaik, R.K. Patel, U. Jha, R.K. Dey, Fluoride removal performance of a new hybrid sorbent of Zr(IV)-ethylenediamine, *Chem. Eng. J.* 184 (2012) 72–81.
- [40] V.S. Mane, I.D. Mall, V.C. Srivastava, Kinetic and equilibrium isotherm studies for the adsorptive removal of brilliant green dye from aqueous solution by rice husk ash, *J. Environ. Manage.* 84 (2007) 390–400.
- [41] B.K. Biswas, J.I. Inoue, K.N. Ghimire, H. Harada, K. Ohoto, H. Kawakita, Adsorptive removal of As(V) and As(III) from water by Zr(IV)-loaded orange waste gel, *J. Hazard. Mater.* 154 (2008) 1066–1074.
- [42] B.K. Biswas, J.I. Inoue, H. Kawakita, K. Ohoto, K. Inoue, Effective removal and recovery of antimony using metal loaded saponified orange waste, *J. Hazard. Mater.* 172 (2009) 721–728.
- [43] G. Zhang, Z. He, W. Xu, A low-cost and high efficient zirconium-modified-Na-attapulgite adsorbent for fluoride removal from aqueous solutions, *Chem. Eng. J.* 183 (2012) 315–324.
- [44] S.M. Maliyekkal, A.K. Sharma, L. Phillip, Manganese-oxide-coated alumina: A promising sorbent for defluoridation of water, *Water Res.* 40 (2006) 3497–3506.
- [45] A. Tor, Removal of fluoride from aqueous solution by using montmorillonite, *Desalination* 201 (2006) 267–276.
- [46] X. Liou, B. Shi, Adsorption of fluoride on zirconium (IV)-impregnated collagen fibre, *Environ. Sci. Technol.* 39 (2005) 4628–4632.

- [47] Y. Ku, H. Chiou, W. Wang, The removal of fluoride ion from aqueous solution by a cation synthetic resin, *Sep. Sci. Technol.* 37 (2002) 89–103.
- [48] N. Viswanathan, S. Meenakshi, Enhanced fluoride sorption using La(III) incorporated carboxylated chitosan beads, *J. Colloid Interface Sci.* 322 (2008) 375–383.
- [49] N. Viswanathan, C.S. Sundaram, S. Meenakshi, Removal of fluoride from aqueous solution using protonated chitosan beads, *J. Hazard. Mater.* 161 (2009) 423–430.
- [50] J. Jimenez-Becerril, M. Solache-Rios, I. Garcia-Sosa, Fluoride removal from aqueous solutions by boehmite, *Water Air Soil Pollut.* 223 (2012) 1073–1078.
- [51] V. Sivasankar, T. Ramachandramoorthy, A. Chandramohan, Fluoride removal from water using activated and MnO₂ coated tamarind fruit (*Tamarindus indica*) shell: Batch and column studies, *J. Hazard. Mater.* 177 (2010) 719–729.